Substrate stiffness modulates gene expression and phenotype in neonatal cardiomyocytes *in vitro*

Giancarlo Forte[1]*, Stefania Pagliari[2], Mitsuhiro Ebara[1], Koichiro Uto[1], Janice Kal Van Tam[1], Sara Romanazzo[2], Carmen Escobedo-Lucea[3,4], Elena Romano[5], Paolo Di Nardo[6], Enrico Traversa[2], Takao Aoyagi[1]

[1]*Biomaterials Unit, International Center for Materials Nanoarchitectonics (MANA), National Institute for Materials Science (NIMS), Tsukuba, Japan.*

[2]*Sustainability Materials Unit, International Center for Materials Nanoarchitectonics (MANA), National Institute for Materials Science (NIMS), Tsukuba, Japan.*

[3]*Comparative Neurobiology Unit, Instituto Cavanilles, University of Valencia- RETICS. Valencia, Spain.*

[4]*Regenerative Medicine Program. Centro de Investigación Principe Felipe, 46012 Valencia, Spain.*

[5]*Department of Biology, University of Rome "Tor Vergata", Italy.*

[6]*Laboratory of Cellular and Molecular Cardiology, Department of Internal Medicine, University of Rome"Tor Vergata", Italy.*

***Correspondence:**
Giancarlo Forte, PhD
Biomaterials Unit,
International Center for Materials Nanoarchitectonics (MANA),
National Institute for Materials Science (NIMS),
1-1 Namiki, Tsukuba
305-0044, Japan
Tel.: +81-29-851-3354 (ext. 8765)
Email: FORTE.Giancarlo@nims.go.jp

G.F. and S.P. equally contributed to this work.

Abstract

Biomaterials to be used as cell delivery systems for cardiac tissue engineering should be able to comply with cardiac muscle contractile activity, while favoring cell survival and neo-angiogenesis in a hostile environment. Biocompatible synthetic materials can be tailored to mimic cardiac tissue three-dimensional organization in the micro- and nanoscale. Nonetheless, they usually display mechanical properties which are far from those of the native myocardium and thus could affect host cell survival and activity. In the present investigation, inert poly-ε-caprolactone (PCL) planar layers were manufactured to change the surface stiffness (with Young modulus ranging from 1 to 133 MPa) without changing matrix chemistry. These substrates were challenged with neonatal murine cardiomyocytes to study the possible effect of substrate stiffness on such cell behavior without changing biological cues. Interestingly, softer substrates (0.91±0.08 MPa and 1.53±0.16 MPa) were found to harbor mostly mature cardiomyocytes having assembled sarcomeres, as shown by the expression of alpha sarcomeric actinin and myosin heavy chain in typical striations and the up-regulation of sarcomeric actin mRNA. On the other hand, a preferential expression of immature cardiac cell genes (Nkx-2.5) and proteins (GATA-4) in cardiac cells grown onto stiffer materials (49.67±2.56 MPa and 133.23±8.67 MPa) was detected. This result could not be ascribed to significant differences in cell adhesion or proliferation induced by the substrates, but to the stabilization of cardiomyocyte differentiated phenotype induced by softer layers. In fact, cardiac cell electromechanical coupling was shown to be more organized on softer surfaces, as highlighted by connexin 43 distribution. Moreover, a differential regulation of genes involved in extracellular matrix remodeling was detected on soft films (0.91±0.08 MPa) as compared to the stiffest (133.23±8.67 MPa). Finally, the up-regulation of a number of genes involved in inflammatory processes was detected when the stiffest polymer is used. These events highlight the differences in cell mechanosensitivity in a heterogeneous cell preparation and are likely to contribute to the differences encountered in cardiac cell phenotype induced by substrate stiffness.

Keywords: cardiac tissue engineering, mechano-biology, cardiomyocytes, substrate stiffness

Running title: Substrate stiffness and cardiomyocyte development

INTRODUCTION

Tissue engineering by means of biodegradable polymers is emerging as a challenging opportunity to treat cardiovascular diseases. The relationships between cells and scaffold chemical and mechano-physical properties are paramount for the definition of safe protocols to transfer tissue engineering techniques to the bedside. In fact, recent reports focused on the opportunity to tune the properties of synthetic substrates to better mimic the features of the tissue of interest, as to provide the cells to be implanted with tissue-specific cues.[1,2] In this context, significant advancements have been recently achieved in the identification of substrate stiffness as one of the key factors in progenitor and stem cell fate determination. [3-7] Moreover, changes in such a substrate property have been also shown to trigger biological responses in several differentiated cell types.[8-10] The transduction of mechanical signals in differentiated as well in undifferentiated cells has been mainly ascribed to the activation of RhoA/ROCK signaling pathway.[11-13] In human mesenchymal stem cells (hMSCs), these signals appear to be integrated by cytoskeleton tension[14] and Ca^{2+} oscillations[15] to foster stem cell determination.

The effects of substrate elasticity on cardiac cells have been addressed by few research groups so far. In embryonic cardiomyocytes, substrate stiffness was shown to affect contractility, with tissue-like Young modulus appearing more suitable for beating activity;[16] consistently, neonatal cardiac cell maturation was demonstrated to be impaired on stiff substrates, while the formation of functional striations in skeletal myotubes was found to be optimal on substrates having a tissue-like stiffness (12 KPa).[17] Nonetheless, the process of cell fusion leading to the formation of myotubes did not seem to be affected by substrate mechanical properties.[18] *In vivo*, the slight variations in substrate stiffness following scar formation after myocardial infarction[19] have been proposed to impair injected or resident stem cell ability to be retained in and repair the injured myocardium,[20-22] while marked differences in ECM rigidity are considered predictive of solid tumor malignancy or progression.[23-25] The ability of living cells to activate specific signaling pathways in response to mechanical stimuli has been recently demonstrated to be highly cell-specific,[4,18,26] this evidence being likely to reflect differences in *in vivo* cell physiology. Given the ability of cells to sense the substrate they grow on and their acknowledged capacity to convert such “feelings” in a biological behavior, one cannot neglect the possibility that scaffolds developed for a specific *in vivo* application could interfere with host cell behavior once they are implanted. In the case of scaffolds to be used in cardiac tissue engineering, they should be able to comply with cardiac contractility,[27] while also representing an easy tool to be handled by the surgeons. Although natural and synthetic

hydrogels represent valuable candidates to mimic cardiac tissue microenvironment in terms of mechano-physical properties,[28] the use of 3D scaffolds allows the control of graft shape and size, as well as the possibility to use the correct number of cells.[29-31] Nonetheless, the possibility that a foreign body reaction could be induced cannot be excluded when synthetic or animal-derived materials are used.[32,33]

A number of natural biomaterials have been so far proposed as scaffolds to treat cardiac pathologies, including alginate, fibrin, collagen, and chitosan.[34-37] Also synthetic derivatives of poly-lactic acid (PLA), poly-ε-caprolactone (PCL) and blends obtained with glycolic acid (PLGA) have been investigated as cell delivery systems for future applications. As a bulk, such materials are known to be far stiffer than myocardium, while microfabrication techniques can be used to obtain an anisotropic distribution of their rigidity. [4,38,39] Aim of the present work is to study the interaction between stiff substrates (from 0.91±0.08 to 133.23±8.67 MPa) and neonatal cardiomyocytes. For this purpose, planar PCL layers displaying different overall stiffness values were obtained by cross-linking tetra-branched PCL with acrylate end-groups in the presence of linear PCL telechelic diacrylates, and tested for their ability to sustain murine neonatal cardiomyocyte adhesion and maturation. Because PCL is a semi-crystalline polymer that has a melting temperature (Tm) over which the mobility of polymer chains changes significantly, the crosslinked PCLs successfully offer branch-structure dependent stiffness without changing the surface wettability. Our results show that softer materials (around 1 MPa stiffness) favor the appearance of cells having correctly oriented sarcomere structure and electromechanical coupling, while the stiffer ones (in the high MPa range) enhance the number of GATA-4-, Nkx-2.5-expressing non-contractile cells, having poor electromechanical coupling and reduced contractile activity. These results could not be ascribed to a differential regulation of cardiac cell adhesion or proliferation by substrate stiffness. Finally, an overall effect of substrate stiffness on cardiac cell gene expression is demonstrated, with genes involved in cell-matrix interaction being up-regulated on the softest substrate, while those related to inflammatory response being significantly activated on the stiffest.

MATERIALS AND METHODS

Poly-ε-caprolactone film preparation and stiffness control

Figure 1 shows a schematic illustration of the PCL materials prepared by cross-linking tetra-branched PCL with acrylate end-groups in the presence of linear PCL telechelicdiacrylates, according to a previously reported protocol.[40] Briefly, two-branched and four-branched PCL were synthesized by ε-caprolactone (CL) ring-opening polymerization that was initiated with tetramethylene glycol and pentaerythritol as initiators, respectively. Then, acryloyl chloride was reacted to the end of the branched chains. The structures and the molecular weights were estimated by ^{1}H NMR spectroscopy (JEOL, Tokyo, Japan) and gel permeation chromatography (JASCO International, Tokyo, Japan). The average degrees of polymerization of each branch on two-branched and four-branched PCL were 18 and 10, respectively. The obtained PCL macromonomers were then dissolved in xylene containing benzoyl peroxide (BPO), and the solution was injected between a glass slide with a 0.2 mm thick Teflon spacer to prepare the substrate layers. The PCL macromonomers were cured for 180 min at 80°C. The mechanical properties of the crosslinked materials were characterized by a tensile test (EZ-S 500N, Shimadzu, Kyoto, Japan). The contact angles on the PCL layers were also determined by a sessile drop method. They were measured 30 seconds after a water drop was placed on the surface at 37°C.

Murine neonatal cardiomyocyte extraction and characterization

The study was performed on neonatal mice under the protocols approved by the institutional Animal Care and Use Committee of the University of Rome Tor Vergata (Rome, Italy). Cardiac cells were extracted from 1/3-day-old neonatal CD1 murine hearts (n = 30) by means of Trypsin enzymatic digestion (0.05% Trypsin in a solution of 0.02% EDTA in phosphate buffer saline (PBS)) for 3 hours at 4°C, followed by incubation in collagenase II (1500 U; Worthington Biochemical Corporation, Lakewood, NJ) for 30 minutes at 37°C. After filtration through a 0.70 μm strainer (Falcon BD, Franklin Lakes, NJ), the samples were collected and centrifuged for 5 minutes at 800xg. Cells were resuspended in Claycomb medium (Sigma-Aldrich, St. Louis, MO) supplemented with 10% fetal bovine serum (FBS, Lonza Group Ltd, Basel, CH), 100 IU/mL penicillin and 4 mM L-glutamine (Sigma-Aldrich) and seeded onto 2 μg/ml fibronectin (BIOCHROM AG, Berlin, Germany)/0.2% laminin in 0.02% gelatin (Sigma-Aldrich) pre-coated tissue culture polystyrene (TCPS) dishes and on PCL planar scaffolds. Cardiac cells were analyzed immediately after the extraction as described below. The number

of beating areas was calculated by counting 10 random fields under light microscope and the mean values obtained from 3 independent experiments reported.

Immunofluorescence staining and confocal microscopy

Cells seeded on TCPS dishes or on PCL layers were fixed with 4% paraformaldehyde in PBS for 30 minutes at 4°C, and permeabilized with 0.1% TritonX-100 (Sigma-Aldrich) in PBS for 2 minutes at room temperature after 1, 3, and 7 day culture. Cells were incubated with antibodies against α-sarcomeric actinin (1:100, Sigma-Aldrich), GATA-4 (1:100, Santa Cruz Biotechnology), ki67 (ABCAM) and myosin heavy chain (MF20-488, eBioscience) for 1 hour at room temperature. The appropriate fluorophore-conjugated secondary antibodies were as follows: Alexa Fluor 488 goat-anti-rabbit and 546 goat-anti-mouse (Invitrogen Corp.). Nuclei were counterstained with 4-6-diamidino-2-phenylindole (DAPI; Sigma-Aldrich). Secondary antibodies in the absence of a specific primary antibody were used to exclude the occurrence of unspecific signals. The images were taken using a Leica DMRB microscope equipped with a digital camera or using a confocal laser scanner microscope (Olympus FV 1000), after excitation at 405 nm, 488 nm, and 543 nm wavelengths for blue, green, and red channels acquisition, respectively. Volume reconstruction (3D rendering) and iso-surface for blue and red channel of xyz confocal image was performed using Imaris software (Bitplane, Zurich).
Cell circle shape factor (or circularity index) was calculated as $4\pi A/P^2$ on acquired images by manually outlining single cardiomyocytes as identified by α-actinin staining (n=30/sample) in ImageJ (National Institute of Health, Bethesda, USA). Cardiomyocyte mean surface area was calculated on α-actinin-positive cells (n=30/sample) by the same method using ImageJ software.

Scanning electron microscopy (SEM) analysis of the samples

Cells grown for 7 days on PCL substrates were fixed in PFA 4% for 15 minutes at room temperature, dried under flow laminar hood and prepared for SEM analysis as previously reported[41] and examined using Hitachi S-4800 low voltage scanning electron microscope.

RNA extraction, real time PCR and PCR array

Total RNA was extracted by TRIZOL Reagent (GIBCO BRL, Gaithersburg, MD). Retrotranscription was carried out with 2 μg of RNA for each sample using reverse transcription (RT) Moloney murine leukemia virus (Invitrogen Corp.) in the presence of random hexamers. Real-time PCR was used to determine the expression profile of 90 key

genes involved in different signal transduction pathways in *Mus musculus*. After synthesis of first-strand cDNAs, RT-PCR (n=3) was performed by the 7500 Real Time PCR System (Applied Biosystems, Foster City, CA) using the RT^2 Profiler PCR Arrays Mouse Signal Transduction Pathway Finder (PAMM-014; Qiagen, Valencia, CA) and Mouse Extracellular Matrix and Adhesion Molecules (PAMM-013A) with the RT^2 SYBR Green/ROX PCR Master mix (Qiagen) according to the manufacturer's protocol. The threshold cycle (Ct) is defined as the fractional cycle number at which the fluorescence reaches 10-fold standard deviation of the baseline (from cycle 3 to 12). The primers used to amplify cardiac-specific genes are the following: Nkx-2.5 (product size: 128) *For:* GAGCCTGGTAGGGAAAGAGC; *Rev:* GAGGGTGGGTGTGAAATCTG: GATA-4 (product size: 78); *For:* GACACACTGCCTTGTCTGGA, *Rev:* GCTGTGATCTGGTCTGAGGTC; Connexin 43 (product size: 74), *For:* AGGATTCAGGGGTAAAGGAAAC *Rev:* GGCTGGGTTGGACAGTTAGT; Alpha cardiac actin (product size: 183) *For:* GTGGCTGGCTTCTCCTCTAA, *Rev:* AACACCTGCTTTCCTTCACAA. The specificity of the SYBR PCR signal was confirmed by melt curve analysis. For the complete list of genes tested, please see Supplementary Table 1.

Statistical analysis

The results are given as mean ± standard deviation as obtained by counting *n* fields per group in three independent experiments. The significance of differences in multi-group comparison was evaluated by one-way analysis of variance (ANOVA) followed by unpaired Student's *t*-test. A final value of $p < 0.05$ was considered statistically significant.

RESULTS:

Preparation of Poly-ε-caprolactone (PCL) layers with controlled stiffness

Cross-linked tetra-branched PCL layers with linear PCL content varying between 0 and 100 wt% were successfully synthesized. As shown in Table 1, tensile tests showed compositionally dependent stiffness ranging from approximately 0.91 MPa to 133.23 MPa, without changing their surface wettability that determine initial cell adhesion in the following experiments (Supplementary Figure 1). Since branch number represents a parameter to adjust crystallinity and mechanical properties of the polymer networks, various suitable combinations can be obtained by simply mixing two- and four-branched macromonomers,. Although the crystallinity of the crosslinked PCLs increased with increasing the two-branched PCL content, the elastic modulus of the layer with 50 wt% of two-branched PCL macromonomer was slightly smaller than that with 0 wt%. This is because the netpoint density within the crosslinked PCL prepared from four-branched macromonomers only was the highest among the samples in this experiment. Thus, the unit length of the PCL macromonomers and netpoint density within the crosslinked PCL structure are the predominant contributors in controlling thermal and mechanical properties. Therefore, the stiffness could be successfully adjusted on demand by precisely tailoring the nano-architecture of semicrystalline PCL, while keeping a cell-compatible surface wettability. The layers displayed stiffness below 1 MPa (0.91±0.08MPa), or in the MPa range (1.53±0.16, 49.67±2.56 and 133.23±8.67 MPa) and comparable surface wettability (Table 1).

Substrate stiffness affects neonatal cardiomyocyte maturation but not adhesion.

Neonatal murine cardiomyocytes were extracted as previously described[7] and seeded onto tissue culture polystyrene (TCPS, virtually infinite stiffness) or PCL layers displaying 0.91±0.08, 1.53±0.16, 49.67±2.56 and 133.23±8.67 MPa stiffness. The number of cells expressing early cardiac commitment marker GATA-4 and mature cardiomyocyte-specific contractile proteins alpha sarcomeric actinin (α–actinin) and cardiac myosin heavy chain was evaluated after 1, 3, and 7 day culture. The presence of α–actinin and myosin in the putative sarcomeric arrangement was considered as a hallmark of differentiated cardiomyocytes (Fig. 2a). No significant differences in the adhesion rate of GATA-4+ cells were noticed 24 h after seeding on the layers having stiffness of 0.91, 1.53, and 49.67 MPa, while a smaller percentage of cells was expressing such marker on the stiffest substrate (133.23 MPa) (Fig. 2b). Nonetheless, after 3 day culture, the number of GATA-4+ cells increased on the stiffer surfaces, the higher percentage being encountered on the layer with 49.67 MPa stiffness (Fig.

2a). A dramatic decrease in GATA-4+ expression was found on all the surfaces after 7 days, apart from the stiffest substrate, where its expression was stable over the culture. On the other hand, the number of α–actinin+ cells decreased in a timely fashion on all the surfaces tested, as expected for terminally differentiated cells[7]. Nonetheless, although the only significant difference in α–actinin+ cell number after 24 h was detected on the 1.53 MPa surface (Fig. 2c), a larger number of positive cells could be found after 3 and 7 days on the softer substrates (0.91 and 1.53 MPa) as compared with the stiffer (49.67, 133.23 MPa, and TCPS). Similar results were obtained by staining myosin heavy chain (data not shown). A thorough quantification of GATA-4+ and α-actinin+ proliferating cells by ki67 expression was performed on the polymers after 3 day culture. The results obtained show that GATA-4 undifferentiated cardiac cells retain a marked ability to proliferate as compared to terminally differentiated α–actinin+ cells, also outlining that no preferential proliferative effect is exerted by the substrates on cardiac cells (Fig. 2d). Cardiomyocytes on TCPS surface showed a similar behavior to those on 133.23 MPa substrate, thus they were excluded from the following experiments.

Cardiomyocyte morphology, sarcomere organization and electromechanical coupling are impaired in long term culture on stiff substrates

As expected, the presence of cells expressing the properly assembled form of sarcomeric protein α–actinin was detected on all the layers tested after 3 day culture, although they appeared to be more scattered on the stiff substrates as compared to the softer, where they were preferentially arranged in clusters (Fig. 3a). At the same time-point, real time PCR performed using primers specific for cardiac markers showed that alpha sarcomeric actin (α sarcomeric actin) expression was enhanced by 1.8 fold on the softest substrate (0.91 MPa), while cardiomyoblast marker GATA-4 resulted upregulated by 1.3 fold on the stiffest (133.23 MPa). A significant downregulation of another marker of cardiomyoblasts, Nkx-2.5, was found on the softest substrate, while only modest changes were detected for the gene encoding for connexin 43 (Fig. 3b). Nonetheless, the contractile apparatus was found disrupted in cardiomyocytes cultured for longer periods (7 days) onto the stiffer surfaces (49.67 and 133.23 MPa), while its pattern was preserved on the softer substrates (0.91 and 1.53 MPa) at the same time-point (Fig. 4a and supplementary figure 2). Additionally, the analysis of cell aspect demonstrated that lower values of circle shape factor and mean surface area (smaller cells with higher aspect ratio) are encountered in cells growing on softer substrates, while those adhering to the stiffer matrix have a higher mean values (bigger cells with low aspect

ratio, Fig. 4c). At the same time-point (7 days), the analysis of connexin 43 distribution within the cells, accounting for electromechanical coupling in fully differentiated cardiomyocytes, demonstrated that a fair membrane distribution could be found on cardiac cells grown onto the softer substrates (0.91 and 1.53 MPa) (Fig. 5a), while it was randomly distributed on the stiffer. The correct distribution of connexin 43 on the softest substrate was also confirmed by 3D rendering at the confocal microscope (Fig. 5a, bottom and supplementary video 1). The same analysis allowed demonstrating functional α–actinin assembly (Fig. 5b) and vinculin expression in cardiomyocytes grown on the softer substrates (Fig. 5c). Cardiomyocyte beating activity was also assessed on the substrates having different overall stiffness, and the beating areas quantified by light microscopy. The number of beating areas in the time-frame considered (1, 3, 4, and 7 days) was found to be significantly higher on the softer substrates (0.91 MPa), while the lowest number of beating areas could be found on the stiffest (133.23 MPa) (Fig. 5d and supplementary videos 2 and 3).

Cardiac cell gene expression is regulated by substrate stiffness

A thorough analysis of gene expression in cardiac cells grown on PCL layers was performed by analyzing 168 genes involved in different signaling pathways and in extracellular matrix formation by PCR array. On this purpose, cardiomyocytes were seeded on 0.91 MPa and 133.23 MPa substrates for 3 days and total RNA extracted. *Ex vivo* extracted cardiomyocytes were used as controls (data not shown). Supplementary figure 3 illustrates a number of genes differentially regulated in cells grown on the films, grouped per function and/or pathway (for complete gene array information, please refer to supplementary table 1). Moreover, figure 6 shows the results of a bioinformatics analysis of gene expression, as obtained by the software GENEMANIA (www.genemania.org). The network in figure 6a demonstrates that the genes up-regulated on 0.91 MPa stiffness are mostly related to cell adhesion (laminins) and extracellular matrix remodeling (MMPs, TIMPs). On the contrary, figure 6b shows that mostly genes involved in the regulation of inflammation response are significantly upregulated on the stiffest substrate (133.23 MPa).

DISCUSSION

The interaction of scaffolds and cells has been so far considered mainly in terms of cell adhesion, proliferation and differentiation,[42] while only in the last few years the possibility that synthetic substrates - designed to provide implanted cells with a favorable microenvironment - could integrate or interfere with cell function *in vivo* has been acknowledged.[43] In fact, at the basis of tissue engineering paradigm lays the idea that a scaffold to be used in tissue regeneration should favor new tissue formation without interfering with organ function.[27] Nonetheless, scaffold physical and mechanical properties have been shown to affect cell survival,[2] proliferation,[44] migration,[5] and eventually differentiation.[3,4] These parameters have been regarded to act cooperatively with biological cues to maintain cell phenotype and function[45] or direct stem cell commitment.[7] Recently, evidence has been given that stem and mature cells can sense the stiffness of the substrate they grow on and perceive this parameter as physiological when it matches tissue-specific values.[3,16] In this context, the indication that embryonic quail and chicken cardiomyocyte beating activity is preserved on scaffolds displaying cardiac-like rigidity appears interesting.[16] Additionally, neonatal rat ventricular cardiomyocytes have been shown to proceed to cell maturation and produce higher mechanical force on matrices having myocardial-like stiffness (10 kPa),[17] while higher values (144 kPa) led to a reduced troponin I staining and poor electrical excitability. Such experiments were justified by the evidence that the local Young modulus for adult rat heart tissue ranges from 11.9 to 46.2 kPa (25.6 ± 15.9 kPa),[46] while infarcted myocardium stiffness has been reported to be around 55±15 kPa in Lewis rats.[19]

The use of synthetic scaffolds having elastomeric properties, being able to comply with the contractile activity of the organ, has been suggested for cardiac tissue repair.[30,47] While synthetic polymers can be easily manufactured to tailor their three-dimensional structure in the nano- and microscale to better reproduce cardiac anisotropy,[4] as a bulk they usually display a Young modulus that is far larger than that measured for body tissues. Among them, poly-ε-caprolactone (PCL) is an elastomeric polyester already approved for biomedical applications by Food and Drug Administration (FDA), and already proven to be suitable for cell culture.[38] Moreover, its longer degradation time as compared to poly-lactide makes it appealing for tissue engineering applications.[48,49]

Thus, in the present investigation, elastomeric poly-ε-caprolactone (PCL) substrates having different Young modulus values (0.91, 1.53, 49.67 and 133.23 MPa) were used to culture neonatal murine cardiac cells and sistematically investigate the effects of substrate stiffness on cardiomyocyte phenotype. Our data show that the expression of a number of genes can be

significantly altered by substrate stiffness in cardiac cells. In particular, genes involved in cell-matrix interaction (lama1, lama2, fn1, vtn, integrins, etc.) and extracellular matrix remodeling (MMPs and TIMPs) were found up-regulated on the softest substrate (0.91 MPa) as compared to the stiffest (133.23 MPa). On the other hand, among the genes found up-regulated on the latter surface, the presence of a number of those involved in immune response control (IL1a, IL2, IL2ra, tnf, fas, fasl, etc.) and inflammatory cell recruitment was detected. These data suggest that in a heterogeneous preparation of cardiac cells obtained from neonatal murine heart, in which cardiomyocytes, cardiac fibroblasts, endothelial, smooth muscle and inflammatory cells are present, those cells can display a cell-specific response to matrix mechanics. Such a concept was already proposed by a number of independent investigations, showing that not all the cells are mechano-sensitive and among those that are able to feel substrate mechanical properties, specific responses can be triggered.[3,4,9,26] Accordingly, the response of heterogeneous cell preparations to substrate mechano-physical properties is likely to be far more complex than what is thought, [3,16] with different cell subsets displaying rather different sensitivity. In this context, the evidence that stiff substrates, in the absence of biological cues, can provoke a raise in immune response appears in good agreement with previous reports showing that the compliance of the microenvironment can interfere with neutrophil migration during the chemotactic process,[50,51] even though our result was obtained using a preparation which is supposed to contain a very limited percentage of inflammatory cells.

As compared to freshly extracted cells, a significant up-regulation of genes involved in cell survival, like *tert*, *Nos2,* and *bax*, occurred when cardiac cells are cultured for 3 days on tissue culture polystyrene (TCPS) dishes, while a concomitant down-regulation of genes responsible for cell proliferation (*jun*, *fos*, *cdk2*, *cdkn1b*, and *egr-1*) was detected in cultured cells in comparison to *ex vivo* cells. Such a gene pattern can be hardly ascribed to a single event (i.e.: ischaemia, hypertrophy, angiogenesis, etc.),[52,53] but it could be compatible with cardiac cell adaptation to the new *in vitro* conditions. Also, differences in cell morphology, phenotype, sarcomere structure and function could be found when cardiomyocytes were cultured on substrates with different stiffness values. In fact, a differential expression of GATA-4, Nkx-2.5, alpha sarcomeric actinin (α-actinin) and myosin heavy chain could be detected. While the number of early cardiomyoblast markers GATA-4- and Nkx-2.5 was found to increase with the substrate stiffness (maximum value on 49.67 and 133.23 MPa surfaces after 1 and 3 days), mature α-actinin-positive cells were positively selected after 3 and 7 days on the softer substrates (0.91 and 1.53 MPa), when a physiological decrease in cardiomyocyte percentage

is expected.[7] Indeed, more than 85% of differentiated cardiomyocytes were retained on the softer surfaces after 3 days as compared to day 1, while only 60% of them could be found on the stiffer substrates. These effects were not mediated by cell adhesion, since the slight differences encountered after 24h culture in GATA-4- and α-actinin-positive cells could not explain such results. Also, these results could not be ascribed to a differential effect of substrate mechanics on cardiac cell proliferation, since no significant differences in proliferating GATA-4- or α-actinin-positive cells could be found on PCL surfaces. Strikingly, a marked difference in the quality of sarcomere structure was noticed at longer time-points (3 and 7 days) as an effect of substrate stiffness. In fact, intact sarcomere bands were retained on softer substrates, while their structure was perturbed in cardiomyocytes grown on the stiffer substrates (49.67-133.23 MPa). Moreover, cardiomyocyte cell shape appeared to be different between the softer and the stiffer substrates, as quantified by circle shape factor and connexin 43 staining, with cells grown on the softer substrates being more elongated and displaying correct electromechanical connections. Consistently, the number of contractile areas after 1, 3, 4, and 7 days after seeding was found to be inversely correlated to the substrate stiffness. Altogether, these data suggest that neonatal cardiomyocytes preferentially acquire and retain a mature phenotype on substrates having Young modulus around 1 MPa, while stiffer surfaces are probably not suitable to sustain their function.

Conclusions

Our data demonstrate that cardiomyocyte phenotype and maturation can be affected by the substrate stiffness and that a higher percentage of mature cardiomyocytes having proper sarcomere assembly, and thus beating activity, can be selected by using substrates having Young modulus around 1 MPa. Nonetheless, the possibility that distinct cell types respond differently to matrix mechanics should be taken into account when scaffolds for a specific application, like cardiac tissue engineering, are to be prepared.

Acknowledgements

The present work was supported by the Japan Society for the Promotion of Science (JSPS) through the “Funding Program for World-Leading Innovative R&D on Science and Technology (FIRST Program)”, and in part by the World Premier International (WPI) Research Center Initiative of MEXT, Japan.

Disclosure statement

The authors have no competing financial interests to disclose.

REFERENCES

1) Freed, L.E., Engelmayr, G.C. Jr, Borenstein, J.T., Moutos, F.T., Guilak, F. Advanced material strategies for tissue engineering scaffolds. Adv Mater **21**, 3410, 2009.

2) Guilak, F., Cohen, D.M., Estes, B.T., Gimble, J.M., Liedtke, W., Chen, C.S. Control of stem cell fate by physical interactions with the extracellular matrix. Cell Stem Cell **5**, 17, 2009.

3) Engler, A.J., Sen, S., Sweeney, H.L., Discher, D.E. Matrix elasticity directs stem cell lineage specification. Cell **126**, 677, 2006.

4) Forte, G., Carotenuto, F., Pagliari, F., Pagliari, S., Cossa, P., Fiaccavento, R., Ahluwalia, A., Vozzi, G., Vinci, B., Serafino, A., Rinaldi, A., Traversa, E., Carosella, L., Minieri, M., Di Nardo, P. Criticatility of the biological and physical stimuli array inducing resident stem cell determination. Stem Cells **26** 2093, 2008.

5) Tse, J.R., Engler, A.J. Stiffness gradients mimicking in vivo tissue variation regulate mesenchymal stem cell fate. PLoS One **e15978**, 2011.

6) Lozoya, O.A., Wauthier, E., Turner, R.A., Barbier, C., Prestwich, G.D., Guilak, F., Superfine, R., Lubkin, S.R., Reid, L.M. Regulation of hepatic stem/progenitor phenotype by microenvironment stiffness in hydrogel models of the human liver stem cell niche. Biomaterials **32**, 7389, 2011.

7) Pagliari, S., Vilela-Silva, A.C., Forte, G., Pagliari, F., Mandoli, C., Vozzi, G., Pietronave, S., Prat, M., Licoccia, S., Ahluwalia, A., Traversa, E., Minieri, M., Di Nardo, P. Cooperation of Biological and Mechanical Signals in Cardiac Progenitor Cell Differentiation. Adv Mater **23**, 514, 2011.

8) Vailhe, B., Ronot, X., Tracqui, P., Usson, Y., Tranqui, L. In vitro angiogenesis is modulated by the mechanical properties of fibrin gels and is related to alpha(v)beta3 integrin localization. In vitro Cell Dev Biol Anim **33**, 763, 1997.

9) Wang, H.B., Dembo, M., Wnag, Y.L. Substrate flexibility regulates growth and apoptosis of normal but not transformed cells. Am J Physiol Cell Physiol **279**, C1345, 2000.

10) Gaca, M.D., Zhou, X., Issa, R., Kiriella, K., Iredale, J.P., Benyon, R.C. Basement membrane-like matrix inhibits proliferation and collagen synthesis by activated rat hepatic stellate cells: evidence for matrix-dependent deactivation of stellate cells. Matrix Biol **22**, 229, 2003.

11) Peyton, S.R., Putnam, A.J. Extracellular matrix rigidity governs smooth muscle cell motility in a biphasic fashion. J Cell Physiol **204**, 198, 2005.

12) Wang, Y.K., Yu, X., Cohen, D.M., Wozniak, M.A., Yang, M.T., Gao, L., Eyckmans, J., Chen, C.S. Bone morphogenetic Protein-2-induced signaling and osteogenesis is regulated by cell shape, RhoA/ROCK, and cytoskeleton tension. Stem Cells Dev DOI:10.1089/scd.2011.0293, 2011.

13) Xu, B., Song, G., Ju, Y., Li, X., Song, Y., Watanabe, S. RhoA/ROCK, cytoskeletal dynamics and focal adhesion kinase are required for mechanical stretch-induced tenogenic differentiation of human mesenchymal stem cells. J Cell Physiol DOI: 10.1002/jcp.23016, 2011.

14) McBeath, R., Pirone, D.M., Nelson, C.M., Bhadriraju, K., Chen, C.S. Cell shape, cytoskeletal tension, and RhoA regulate stem cell lineage commitment. Dev Cell **6**, 483, 2004.

15) Kim, T.J., Seong, J., Ouyang, M., Sun, J., Lu, S., Hong, J.P., Wang, N., Wang, Y. Substrate rigidity regulates Ca2+ oscillation via RhoA pathway in stem cells. J Cell Physiol **218**, 285, 2009.

16) Engler, A.J., Carag-Krieger, C., Johnson, C.P., Raab, M., Tang, H.Y., Speicher, D.W., Sanger, J.W., Sanger, J.M., Discher, D.E. Embryonic cardiomyocytes beat best on a matrix with heart-like elasticity: scar-like rigidity inhibits beating. J Cell Sci **121**, 3794, 2008.

17) Jacot, J.G., McCulloch, A.D., Omens, J.H. Substrate stiffness affects the functional maturation of neonatal rat ventricular myocytes. Biophys J **95**, 3479, 2008.

18) Engler, A.J., Griffin, M.A., Sen, S., Bönnemann, C.G., Sweeney, H.L., Discher, D.E. Myotubes differentiate optimally on substrates with tissue-like stiffness: pathological implications for soft or stiff microenvironments. J Cell Biol **166**, 877, 2004.

19) Berry, M.F., Engler, A.J., Woo, Y.J., Pirolli, T.J., Bish, L.T., Jayasankar, V., Morine, K.J., Gardner, T.J., Discher, D.E., Sweeney, H.L. Mesenchymal stem cell injection after myocardial infarction improves myocardial compliance. Am J Physiol Heart Circ Physiol **290**, H2196, 2006.

20) Wang, X., Hu, Q., Nakamura, Y., Lee, J., Zhang, G., From, A.H., Zhang, J. The role of the sca-1+/CD31- cardiac progenitor cell population in postinfarction left ventricular remodeling. Stem Cells **24**, 1779, 2006.

21) Breitbach, M., Bostani, T., Roell, W., Xia, Y., Dewald, O., Nygren, J.M., Tienmann, K., Bohlen, H., Hescheler, J., Welz, A., Bloch, W., Jacobsen, S.E., Fleischmann, B.K. Potential risks of bone marrow cell transplantation into infarcted hearts. Blood **110**, 1362, 2007.

22) Den Haan, M., Grauss, R.W., Smits, A.M., Winter, E.M., van tuyn, J., Pijnappels, D.A., Steendijk, P., Gittenberger-DeGroot, A.C., van der Laarse, A., Fibbe, W.E., de Vries, A.A., Schalij, M.J., Doevendans, P.A., Goumans, M.J., Atsma, D.E. Cardiomyogenic differentiation-independent improvement of cardiac function by human cardiomyocyte progenitor cell injection in ischemic mouse hearts. J Cell Mol Med. DOI: 10.1111/j.1582-4934.2011.01468.x. 2011.

23) Swaminathan, V., Mythreye, K., O'Brien, E.T., Berchuck, A., Blobe, G.C., Superfine, R. Mechanical stiffness grades metastatic potential in patient tumor cells and in cancer cell lines. Cancer Res **71**, 5075, 2011.

24) Indra, I., Beningo, K.A. An in vitro correlation of metastatic capacity, substrate rigidity, and ECM composition. J Cell Biochem **112**, 3151, 2011.

25) Liang, Y., Jeong, J., De Volder, R.J., Cha, C., Wang, F., Tong, Y.W., Kong, H. A cell-instructive hydrogel to regulate malignancy of 3D tumor spheroids with matrix rigidity. Biomaterials **32**, 9308, 2011.

26) Georges, P.C., Janmey, P.A. Cell type-specific response to growth on soft materials. J Appl Physiol **98**, 1547, 2005.

27) Forte, G., Pagliari, S., Pagliari, F., Ebara, M., Di Nardo, P., Aoyagi, T. Towards the generation of patient-specific patches for cardiac repair. Stem Cell Rev DOI: 10.1007/s12015-011-9325-8. 2011.

28) Li, Z., Guan, J. Hydrogels for cardiac tissue engineering. Polymers **3**, 740, 2011.

29) Chen, Q-Z., Bismarck, A., Hansen, U., Junaid, S., Tran, M.Q., Harding, S.E., Ali, N.N., Boccaccini, A.R. Characterisation of a soft elastomer poly(glycerol sebacate) designed to match the mechanical properties of myocardial tissue. Biomaterials **29**, 47, 2008.

30) Engelmayr, G.C. Jr, Cheng, M., Bettinger, C.J., Borenstein, J.T., Langer, R., Freed, L.E. Accordion-like honeycombs for tissue-engineering of cardiac anisotropy. Nat Mater **7**, 1719, 2008.

31) Di Nardo, P., Forte, G., Ahluwalia, A., Minieri, M. Cardiac progenitor cells: potency and control. J Cell Physiol **224**, 590, 2010.

32) Badylak, S.F., Gilbert, T.W. Immune response to biologic scaffold materials. Semin Immunol **20**, 109, 2008.

33) Di Felice, V., De Luca, A., Serradifalco, C., Di Marco, P., Verin, L., Motta, A., Guercio, A., Zummo, G. Adult stem cells, scaffolds for in vivo and in vitro myocardial tissue engineering. Ital J Anat Embryol **115**, 65, 2010.

34) Leor, J., Aboulafia-Etzion, S., Dar, A., Shapiro, L., Barbash, I.M., Battler, A., Granot, Y., Cohen, S. Bioengineered cardiac grafts – a new approach to repair the infarcted myocardium? Circulation **102**, 56, 2000.

35) Li, R.K., Yau, T.M., Weisel, R.D., Mickle, D.A.G., Sakai, T., Sakai, T., Choi, A., Jia, Z.Q. Construction of a bioengineered cardiac graft. J Thorac Cardiovasc Surg **119**, 368, 2000.

36) Jockenhoevel, S., Zund, G., Hoerstrup, S.P., Chalabi, K., Sachweh, J.S., Demircan, L., Messmer, B.J., Turina, M. Fibrin gel – advantages of a new scaffold in cardiovascular tissue engineering. Eur J Cardiothorac Surg **19**, 424, 2001.

37) Blan, N.R., Birla, R.K. Design and fabrication of heart muscle using scaffold-based tissue engineering. J Biomed Mater Res A **86**, 195, 2008.

38) Soliman, S., Pagliari, S., Rinaldi, A., Forte, G., Fiaccavento, R., Pagliari, F., Minieri, M., Di Nardo, P., Licoccia, S., Traversa, E. Multiscale 3D Scaffolds for Soft Tissue Engineering via Multimodal Electrospinning. Acta Biomater **6**, 1227, 2010.

39) Mariani, M., Rosatini, F., Vozzi, G., Previti, A., Ahluwalia, A. Characterization of tissue-engineered scaffolds microfabricated with PAM. Tissue Eng **12**, 547, 2006.

40) Ebara, M., Uto, K., Idota, N., Hoffman, J.M., Aoyagi, T. Shape-memory surface with dynamically tunable nano-geometry activated by body heat. Adv Mater DOI: 10.1002/adma.201102181. 2011.

41) Mandoli, C., Pagliari, F., Pagliari, S., Forte, G., Di Nardo, P., Licoccia, S., Traversa, E. Stem cell aligned growth induced by CeO_2 nanoparticles in PLGA scaffolds with improved bioactivity for regenerative medicine. Adv Funct Mater **20**, 1617, 2010.

42) Janmey, P.A., Miller, R.T. Mechanisms of mechanical signaling in development and disease. J Cell Sci **124**, 9, 2011.

43) Leor, J., Amsalem, Y., Cohen, S. Cells, scaffolds, and molecules for myocardial tissue engineering. Pharmacol Ther **105**, 151, 2005.

44) Kress, S., Neumann, A., Weyand, B., Kasper, C. Stem Cell Differentiation Depending on Different Surfaces. Adv Biochem Eng Biotechnol 2011 Nov 9.[Epub ahead of print].

45) Nadzir, M.M., Kino-Oka, M., Maruyama, N., Sato, Y., Kim, M.H., Sugawara, K., Taya, M. Comprehension of terminal differentiation and dedifferentiation of chondrocytes during passage cultures. J Biosci Bioeng **112**, 395, 2011.

46) Bhana, B., Lyer, R.K., Chen, W.L., Zhao, R., Sider, K.L., Likhitpanichkul, M., Simmons, C.A., Radisic, M. Influence of substrate stiffness on the phenotype of heart cells. Biotechnol Bioeng **105**, 1148, 2010.

47) Vunjak-Novakovic, G., Tandon, N., Godier, A., Maidhof, R., Marsano, A., Martens, T.P., Radisic, M. Challenges in cardiac tissue engineering. Tissue Eng Part B Rev **16**, 169, 2010.

48) Sung, H-J., Meredith, C., Johnson, C., Galis, Z.S. The effect of scaffold degradation rate on three-dimensional cell growth and angiogenesis. Biomaterials **25**, 5735, 2004.

49) Sun, H., Mei, L., Song, C., Cui, X., Wang, P. The *in vivo* degradation, absorption and excretion of PCL-based implant. Biomaterials **27**, 1735, 2006.

50) Oakes, P.W., Patel, D.C., Morin, N.A., Zitterbat, D.P., Fabry, B., Reichner, J.S., Tang, J.X. Neutrophil morphology and migration is affected by substrate elasticity. Blood **114**, 1387, 2009

51) Jannat, R.A., Dembo, M., Hammer, D.A. Neutrophil adhesion and chemotaxis depend on substrate mechanics. J Phys Condens Matter **22**, 194117, 2010

52) Khachighian, L.M. Early growth response-1 in cardiovascular pathology. Circ Res **98**, 186, 2006.

53) Eguchi, M., Liu, Y., Shin, E.J., Sweeney, G. Leptin protects H9c2 rat cardiomyocytes from H2O2-induced apoptosis. FEBS Journal **275**, 3136, 2008.

Figure captions:

FIG. 1. Schematic illustration of preparation of cross-linked PCLs. Layers with various stiffness were obtained by simply mixing and curing two- and four-branched PCL with acrylate end-groups. PCL macromonomers were dissolved in xylene containing benzoyl peroxide (BPO), cured for 180 min at 80°C and the solution injected between a glass slide with a 0.2 mm thick Teflon spacer to obtain planar layers.

TABLE 1. Mechanical properties and surface wettability of layers made of cross-linked PCLs. The mechanical properties at 37°C were characterized by a tensile test. The contact angles on the films were determined by a sessile drop method. Compositionally dependent stiffness values were achieved, while keeping the surface wettability constant.

FIG. 2. Substrate stiffness affects neonatal cardiomyocyte maturation but not adhesion or proliferation**.** Murine neonatal cardiomyocytes were cultured onto PCL substrates having 0.91, 1.53, 49.67 and 133.23 MPa stiffness and tissue culture polystyrene (TCPS, virtually infinite stiffness) for 1, 3, and 7 days. The presence of fully differentiated cardiomyocytes within the preparations was assessed by co-staining alpha sarcomeric actinin (red) and myosin heavy chain (myosin, green) in the typical striations (**A**). GATA-4 staining accounts for the presence of immature cardiomyocytes and non-myocytes (**B**), while alpha sarcomeric actinin (α-actinin) decoration shows the percentage of cardiomyocytes displaying assembled sarcomere structure (**C**) on substrates having different stiffness values. The presence of proliferating cells among GATA-4+ or α-actinin+ cells was evaluated by ki67 co-staining after 3 day culture on the different polymers (**D**). *, $p<0.05$ after 1 day culture; **, $p<0.05$ after 7 day culture (n= 9).

FIG. 3. Neonatal cardiomyocytes express coherent sarcomere banding in short-term culture on substrates with different stiffness values. Neonatal cardiomyocytes cultured for 3 days onto substrates having stiffness below 1 MPa (0.91 MPa) or in the MPa range (1.53, 49.63, 133.23 MPa) display sarcomere banding, as highlighted by α-actinin staining (red). Nuclei are counterstained in blue (DAPI) (**A**). At the same time-point, Real Time PCR analysis was performed using primers specific for markers alpha sarcomeric actin, connexin 43, GATA-4 and Nkx-2.5 on cardiac cells cultured on PCL substrates as compared to tissue culture polystyrene (TCPS) dishes (**B**). The results are representative of three independent experiments. *, $p<0.05$.

FIG. 4. Long term culture of neonatal cardiomyocytes discloses differences in cell response to substrate stiffness. Sarcomeric actinin (α–actinin, red) staining of neonatal cardiac cells grown for 7 days onto substrates having different stiffness values shows that the contractile apparatus is perturbed in cells growing onto stiff matrix (133.23 MPa), while on softer substrates (0.9, 1.53 MPa) sarcomeric striations are still well organized (**A**). The insets show a higher magnification of the sarcomeric structure. SEM micrographs confirm the presence of cells having correct sarcomeric organization on the softest substrate (**B**). In the bottom

picture, arrowheads indicate the sarcomere. Also, cells grown on substrates having different stiffness values display rather different shapes, as measured by circle shape factor, and different mean area (**C**). In fact, cells on stiffer substrates acquire a flat morphology, with a higher circle shape factor and mean surface area (**C**). Circle shape factor and mean cardiomyocyte area were calculated by manually outlining α-actinin-positive cells in ImageJ (n=50/each sample). The results are reported as mean±S.D. Dashed lines are guide for the eyes.

FIG. 5. Substrate stiffness perturbs cardiomyocyte electro-mechanical coupling. Connexin 43 staining (red) - accounting for cell-to-cell interaction and electromechanical coupling in cardiomyocytes – appears functionally expressed on cell membrane in cardiomyocytes grown onto softer (0.91 and 1.53 MPa) substrates for 7 days, while its expression is scattered in those cultured onto stiffer (49.63 and 133.23 MPa) substrates at the same time point (**A**). The appropriateness of connexin 43 expression on softer substrates is confirmed in 3D confocal images (**A**, bottom). A representative image highlighting α-actinin staining (red) in cardiomyocytes grown for 7 days onto 0.91 MPa surface and its 3D confocal reconstruction (**B**). Functional cell-substrate interactions are present on soft substrates (0.91 MPa), as demonstrated by vinculin staining (red) and its 3D confocal reconstruction (**C**). Nuclei are counterstained with DAPI (blue). The occurrence of spontaneous beating areas within cardiomyocyte culture on the substrates tested demonstrated that a significantly higher number of beating areas could be found onto the softer (0.91 and 1.53 MPa) substrates, as compared to the stiffer (49.63 and 133.23 MPa). This evidence was confirmed after 1, 3, 4 and 7 days in culture (**D**).

FIG. 6. Gene expression regulation by substrate stiffness in murine neonatal cardiomyocytes. Computational gene analysis obtained by plotting in GENEMANIA software (www.genemania.org) the results of two PCR array sets containing 186 genes of interest in cardiac cells grown for 3 days onto PCL layers having 0.91 (**A**) and 133.23 (**B**) MPa stiffness. Only genes differentially regulated on any of the two polymers are plotted (for the complete list of genes tested, please refer to supplementary table 1). Networks legend highlights the presence of physical interactions, co-expression or co-localization of the products of the genes differentially regulated. Functions legend underlines the participation of the gene products differentially regulated to specific molecular pathways.

Supplementary Material:

Supplementary FIG. 1. Stress/strain curves for PCL polymers obtained by mixing four branched and two branched PCL macromonomers at different concentrations (100/0, 50/50, 30/70 and 0/100), as obtained by tensile test.

Supplementary TABLE 1. Complete list of the genes tested in murine neonatal cardiomyocytes cultured for 3 days on PCL layers having 0.91 or 133.23 MPa Young modulus.

The genes up-regulated on the stiff (133.23 MPa, blue) or on the soft (0.91 MPa, red) layer are indicated. Value threshold is set at 2.

Supplementary FIG. 2. Expression of sarcomeric proteins actinin (red) and myosin (green) in cardiomyocytes grown for 7 days onto polymers having different stiffness. Nuclei are counterstained with DAPI (blue). Please note the disruption of sarcomeric structure on the stiff layers.

Supplementary FIG. 3. Genes significantly regulated on 0.91 MPa layers as compared to 133.23 MPa. The involvement of the genes to specific signaling pathways is indicated.

Supplementary VIDEO 1. 3D rendering of connexin 43 expression (red) in neonatal murine cardiomyocytes grown for 7 days on PCL surface having 0.91 overall stiffness. Nuclei are counterstained with DAPI (blue).

Supplementary VIDEO 2. Representative video of beating cardiomyocytes onto PCL surfaces having 49.67 MPa Young Modulus. The video was taken at day 3.

Supplementary VIDEO 3. Representative video of beating cardiomyocytes onto PCL surfaces having 0.91 MPa Young Modulus. The video was taken at day 3.

Figure 1

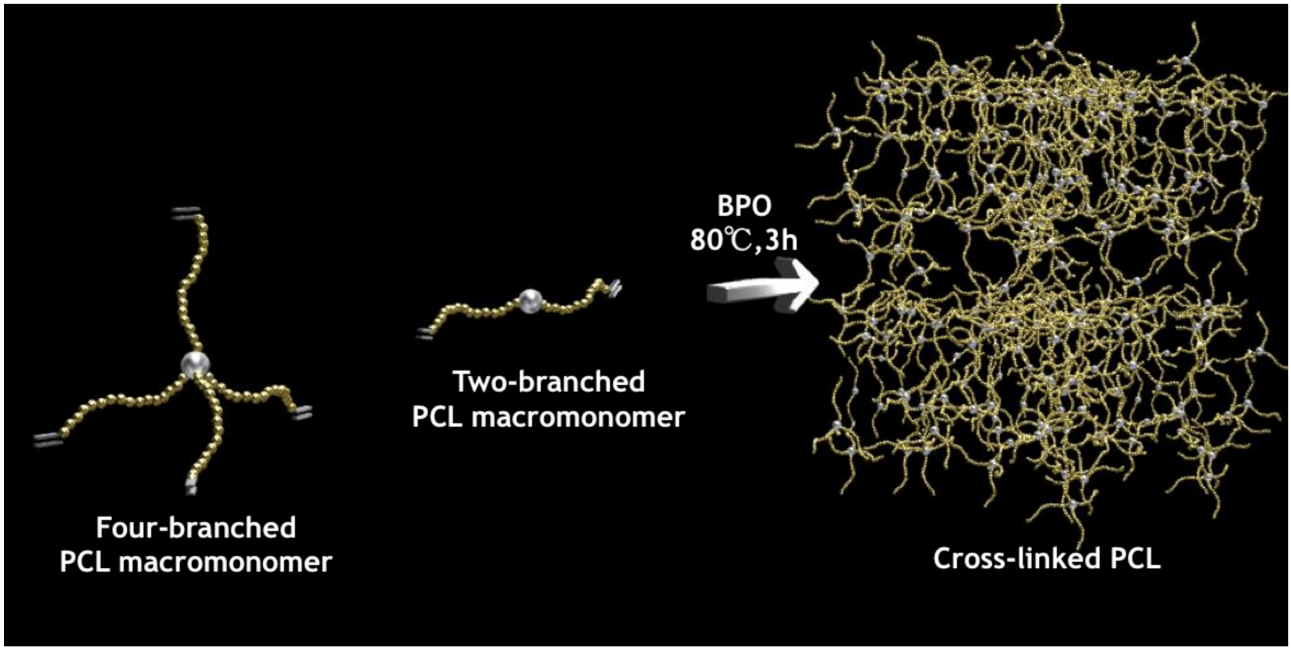

Table 1

Composition of 4-/2-branched PCL (wt%)	Characterization at 37°C	
	Elastic modulus (MPa)	Contact angle (°)
100/0	1.53 ± 0.16	97.4 ± 2.4
50/50	0.91 ± 0.08	98.7 ± 1.6
30/70	49.67 ± 2.56	97.1 ± 3.0
0/100	133.23 ± 8.67	97.7 ± 3.1

Figure 2

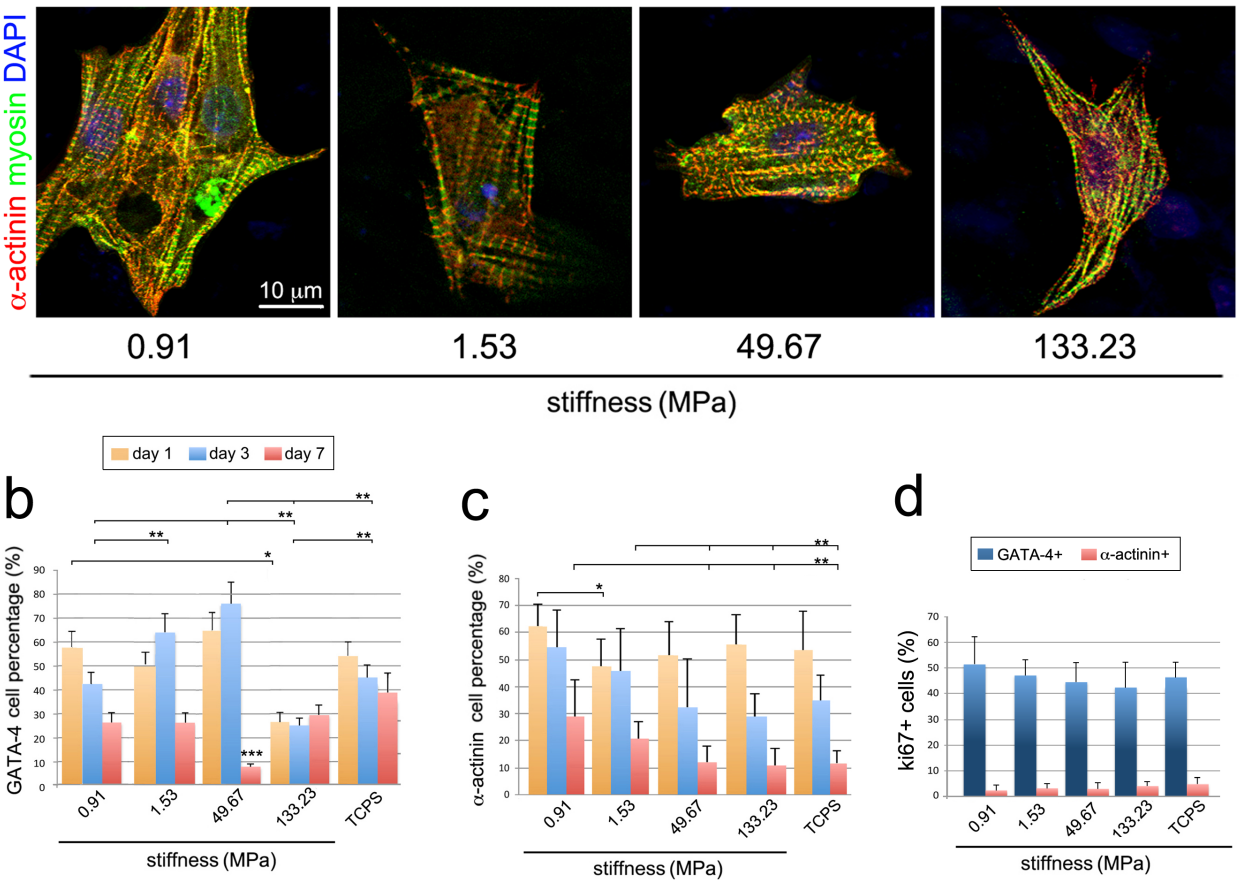
a
α-actinin myosin DAPI
10 μm
0.91
1.53
49.67
133.23
stiffness (MPa)
day 1
day 3
day 7
b
GATA-4 cell percentage (%)
0.91
1.53
49.67
133.23
TCPS
stiffness (MPa)
c
α-actinin cell percentage (%)
stiffness (MPa)
d
GATA-4+
α-actinin+
ki67+ cells (%)
stiffness (MPa)

Figure 3

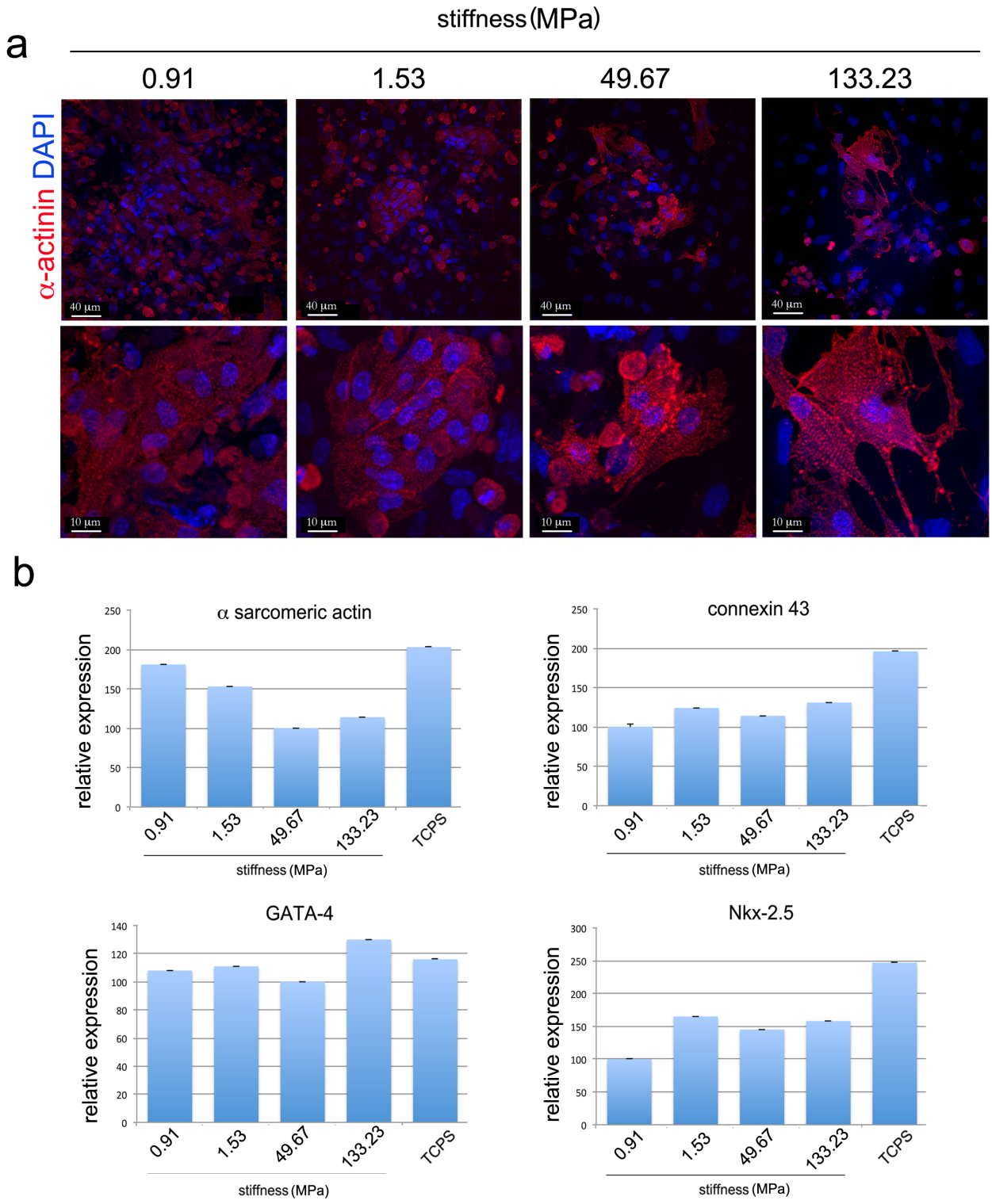
a
stiffness (MPa)
0.91
1.53
49.67
133.23
α-actinin DAPI
40 μm
10 μm
b
α sarcomeric actin
connexin 43
GATA-4
Nkx-2.5
relative expression
stiffness (MPa)
0.91
1.53
49.67
133.23
TCPS

Figure 4

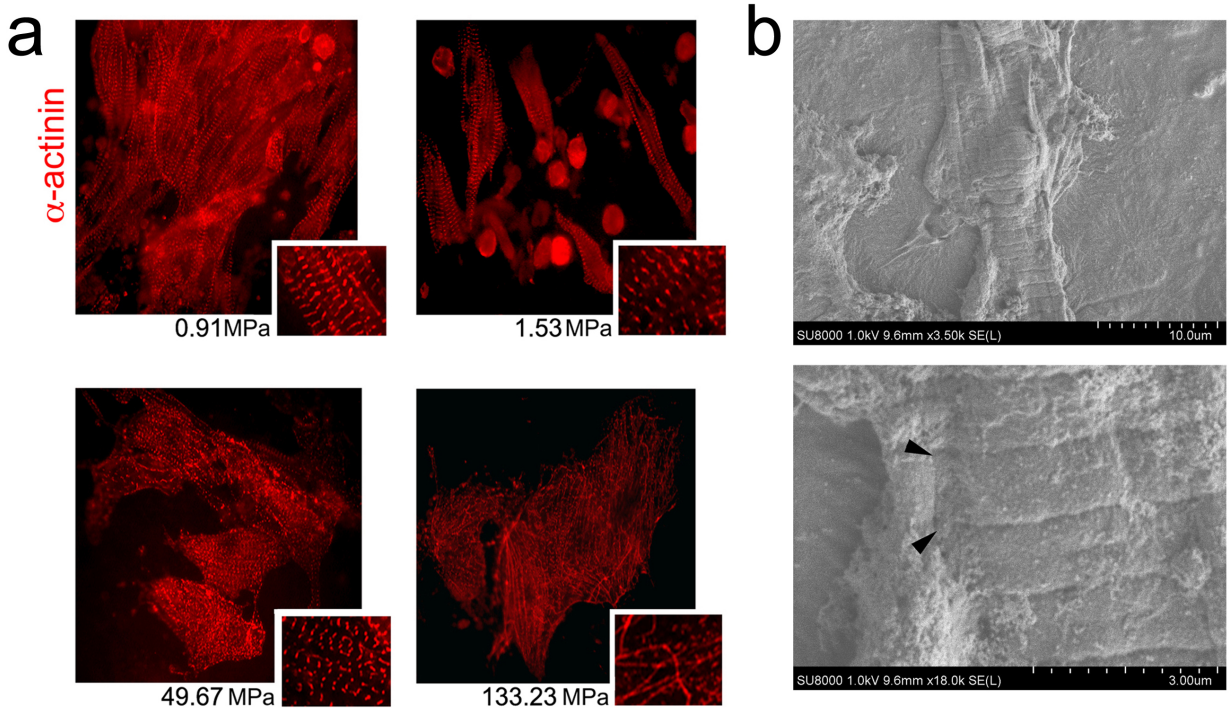
a
α-actinin
0.91MPa
1.53MPa
49.67 MPa
133.23 MPa
b
SU8000 1.0kV 9.6mm x3.50k SE(L)
10.0um
SU8000 1.0kV 9.6mm x18.0k SE(L)
3.00um

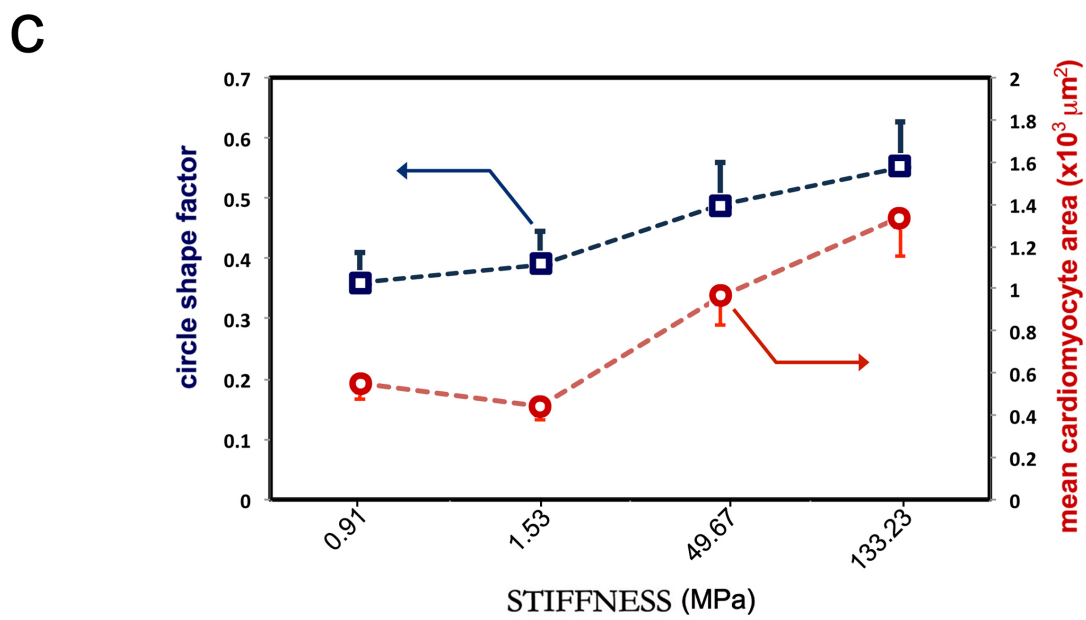
c
circle shape factor
mean cardiomyocyte area (x10³ μm²)
0.7
0.6
0.5
0.4
0.3
0.2
0.1
0
2
1.8
1.6
1.4
1.2
1
0.8
0.6
0.4
0.2
0
0.91
1.53
49.67
133.23
STIFFNESS (MPa)

Figure 5

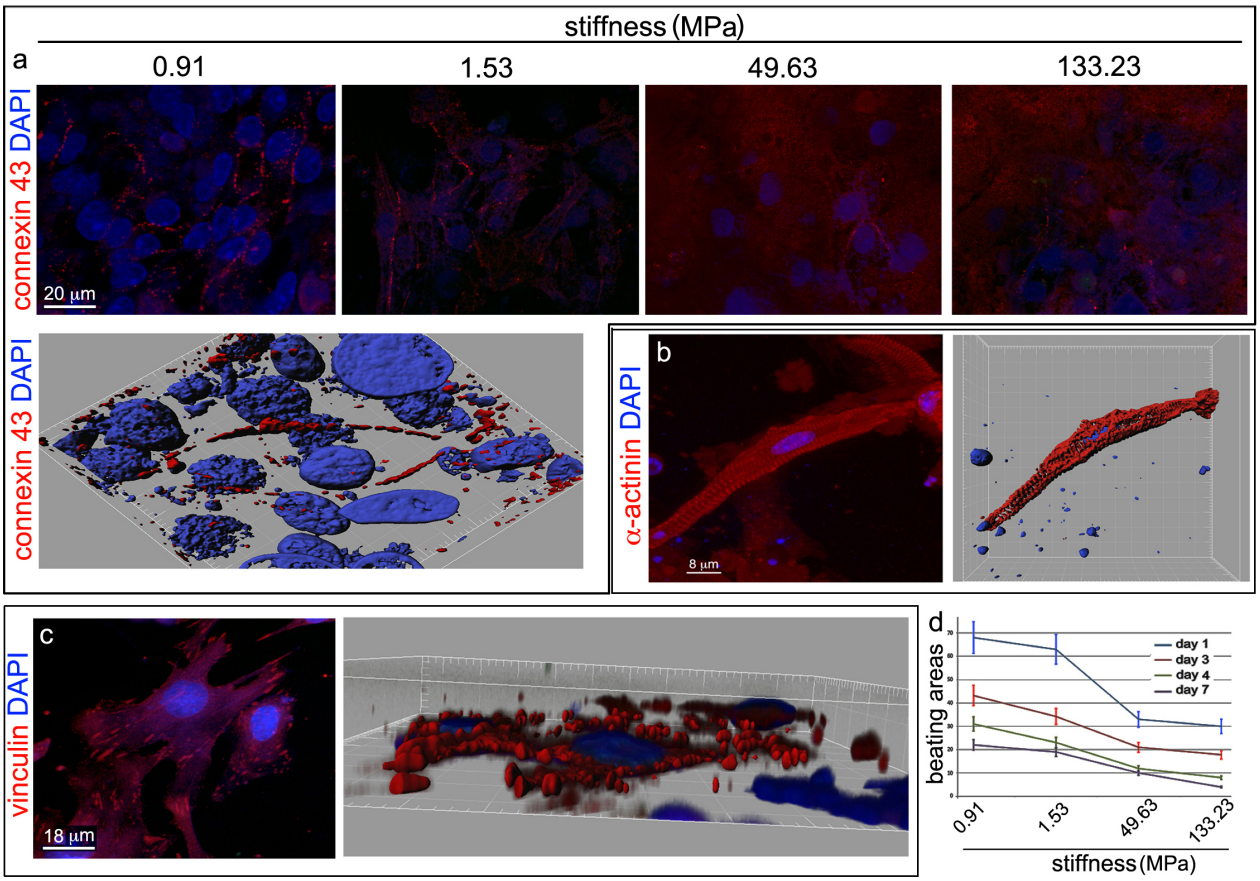
stiffness (MPa)
a
0.91
1.53
49.63
133.23
connexin 43 DAPI
20 μm
connexin 43 DAPI
b
α-actinin DAPI
8 μm
c
vinculin DAPI
18 μm
d
beating areas
day 1
day 3
day 4
day 7
0.91
1.53
49.63
133.23
stiffness (MPa)

Figure 6

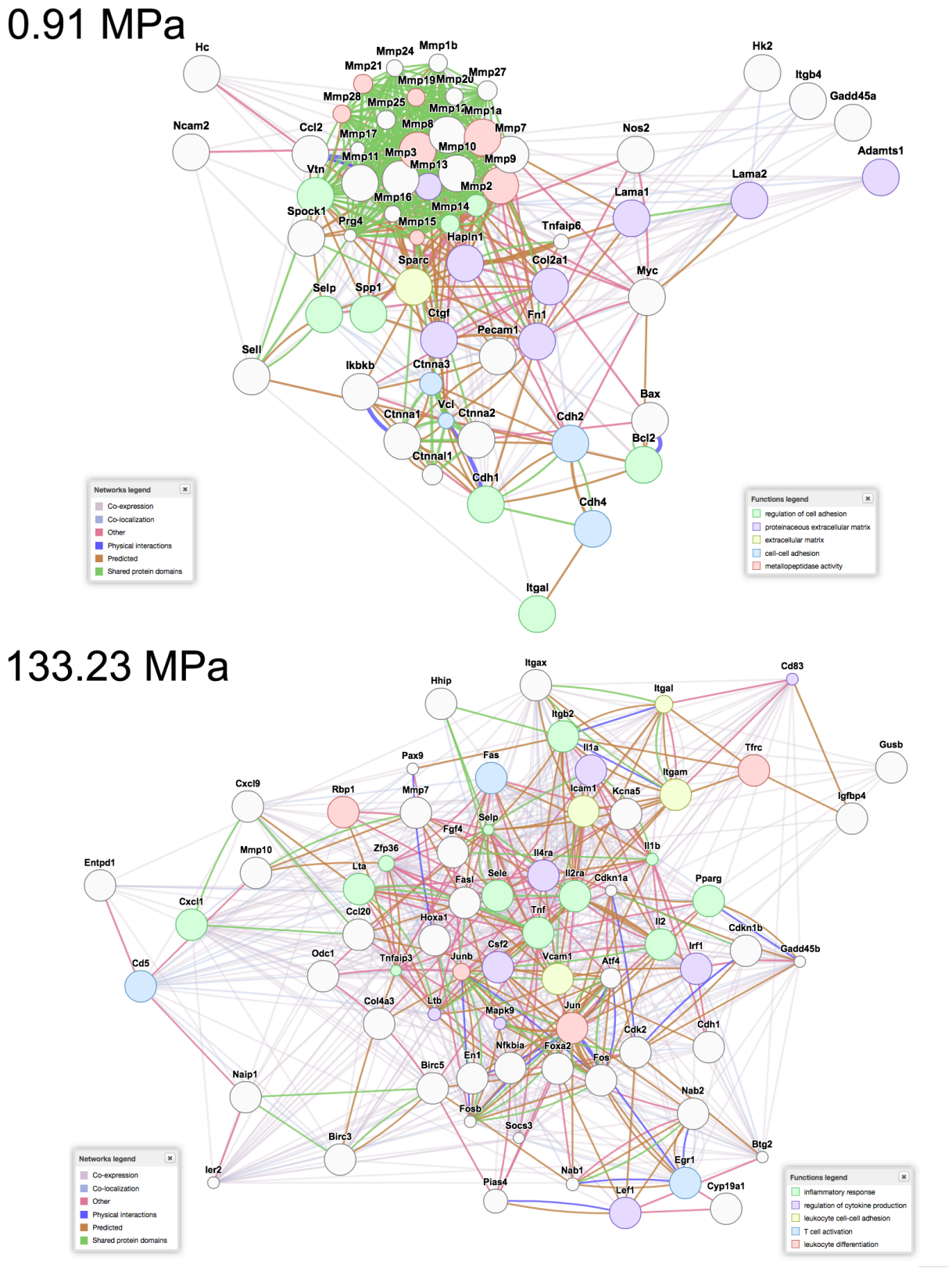
0.91 MPa
Hc
Mmp24
Mmp1b
Mmp21
Mmp27
Mmp19
Mmp2u
Mmp28
Mmp25
Mmp12
Mmp1a
Ncam2
Ccl2
Mmp8
Mmp7
Mmp17
Mmp10
Mmp3
Mmp11
Mmp9
Vtn
Mmp13
Mmp2
Mmp16
Mmp14
Spock1
Prg4
Mmp15
Hapln1
Tnfaip6
Sparc
Col2a1
Selp
Spp1
Ctgf
Fn1
Pecam1
Sell
Ikbkb
Ctnna3
Vcl
Ctnna1
Ctnna2
Ctnnal1
Cdh1
Cdh4
Itgal
Hk2
Itgb4
Gadd45a
Adamts1
Nos2
Lama2
Lama1
Myc
Bax
Bcl2
Cdh2
Networks legend
Co-expression
Co-localization
Other
Physical interactions
Predicted
Shared protein domains
Functions legend
regulation of cell adhesion
proteinaceous extracellular matrix
extracellular matrix
cell-cell adhesion
metallopeptidase activity
133.23 MPa
Itgax
Hhip
Cd83
Itgal
Itgb2
Il1a
Tfrc
Gusb
Pax9
Fas
Itgam
Cxcl9
Rbp1
Mmp7
Icam1
Kcna5
Igfbp4
Selp
Fgf4
Il1b
Mmp10
Zfp36
Il4ra
Entpd1
Lta
Fasl
Sele
Il2ra
Cdkn1a
Pparg
Cxcl1
Ccl20
Tnf
Hoxa1
Il2
Cdkn1b
Csf2
Irf1
Gadd45b
Odc1
Tnfaip3
Junb
Vcam1
Atf4
Cd5
Col4a3
Ltb
Mapk9
Jun
Cdk2
Cdh1
Nfkbia
Foxa2
En1
Fos
Birc5
Naip1
Nab2
Fosb
Socs3
Birc3
Btg2
Ier2
Nab1
Egr1
Pias4
Lef1
Cyp19a1
Networks legend
Co-expression
Co-localization
Other
Physical interactions
Predicted
Shared protein domains
Functions legend
inflammatory response
regulation of cytokine production
leukocyte cell-cell adhesion
T cell activation
leukocyte differentiation

Supplementary figure 1

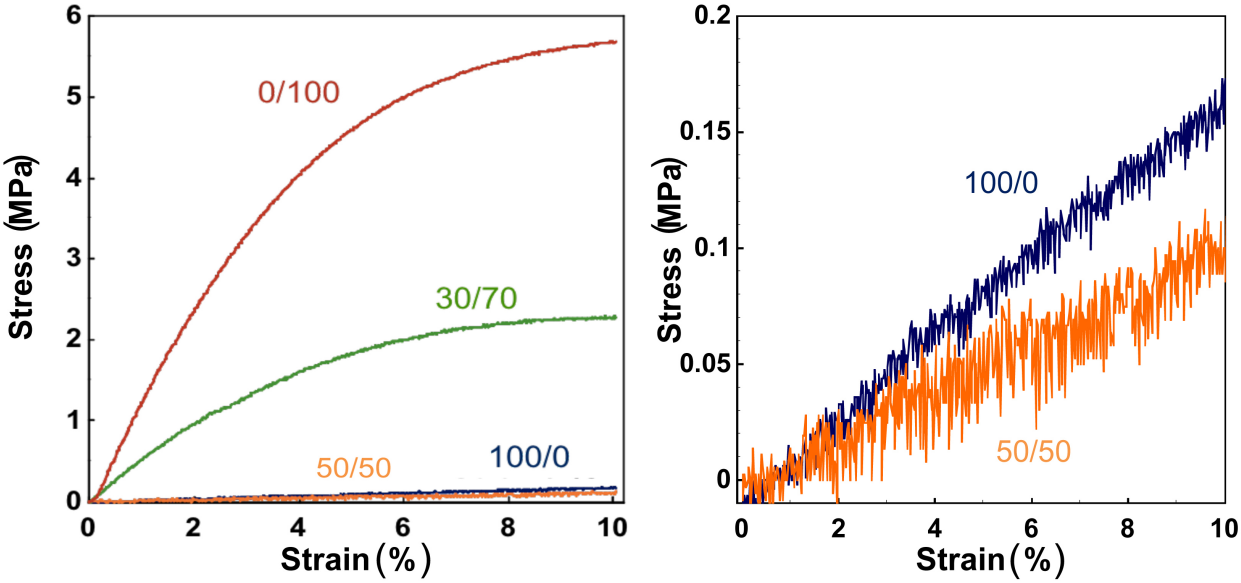

Supplementary figure 2

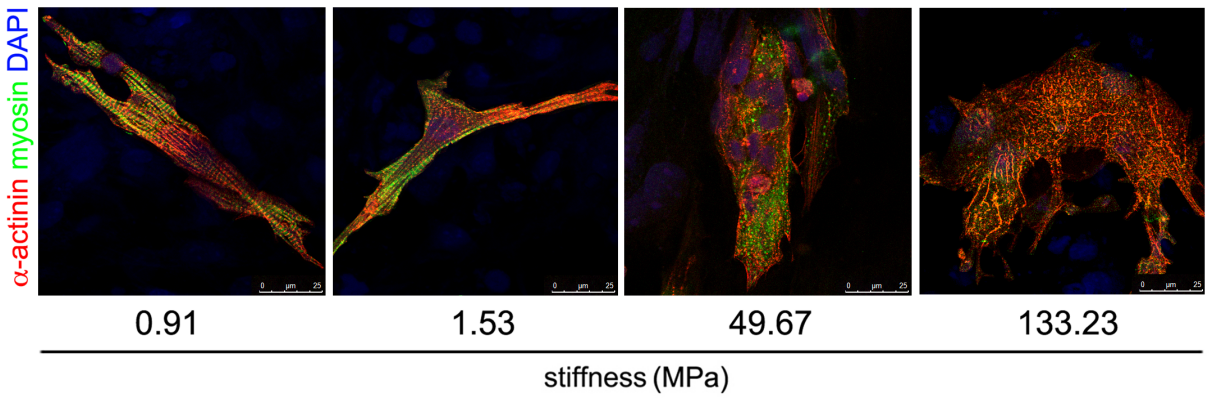

Supplementary Figure 3

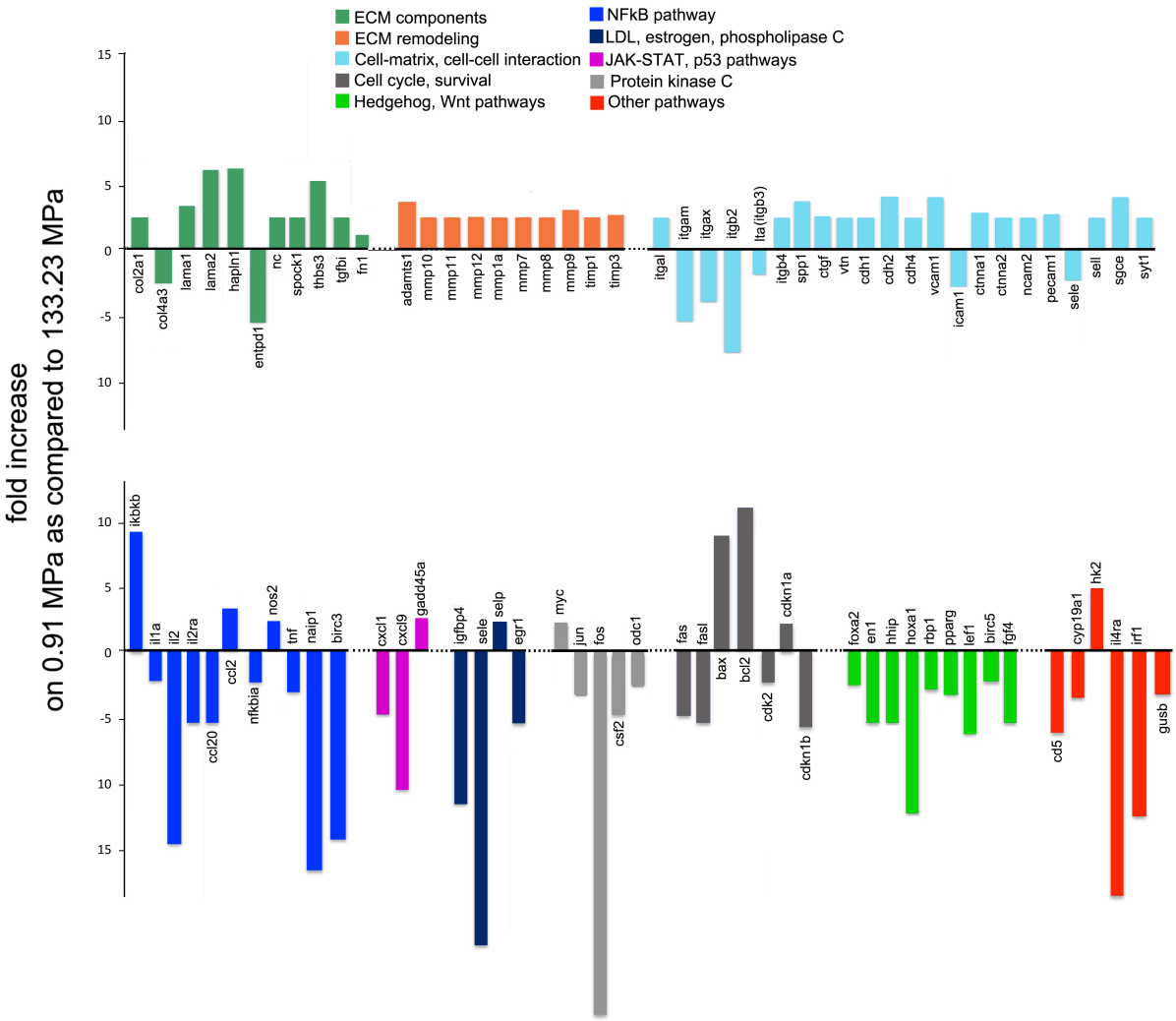

Supplementary table 1

Gene	Gene Regulation on 0.91 MPa (as compared to 133.23 MPa)		
	Fold Regulation	Unigene	Refseq
Adamts1	3.1427	Mm.1421	NM_009621
Adamts2	1.1745	Mm.339048	NM_175643
Adamts5	1.3305	Mm.112933	NM_011782
Adamts8	1.8687	Mm.100582	NM_013906
Ctnna1	2.4318	Mm.18962	NM_009818
Ctnna2	2.0734	Mm.34637	NM_009819
Ctnnb1	-1.1712	Mm.291928	NM_007614
Cd44	1.7802	Mm.423621	NM_009851
Cdh1	2.0734	Mm.35605	NM_009864
Cdh2	3.5113	Mm.257437	NM_007664
Cdh3	1.5497	Mm.4658	NM_001037809
Cdh4	2.0734	Mm.184711	NM_009867
Cntn1	-1.1471	Mm.470343	NM_007727
Col1a1	-1.264	Mm.277735	NM_007742
Col2a1	2.0734	Mm.2423	NM_031163
Col3a1	-1.1313	Mm.249555	NM_009930
Col4a1	-1.1313	Mm.738	NM_009931
Col4a2	-1.2816	Mm.181021	NM_009932
Col4a3	-2.4419	Mm.389135	NM_007734
Col5a1	1.0439	Mm.7281	NM_015734
Col6a1	1.0585	Mm.2509	NM_009933
Vcan	-1.0483	Mm.158700	NM_001081249
Ctgf	2.1615	Mm.390287	NM_010217
Ecm1	-1.2041	Mm.3433	NM_007899
Emilin1	-1.452	Mm.286375	NM_133918
Entpd1	-5.1266	Mm.2824	NM_009848
Fbln1	1.8302	Mm.297992	NM_010180
Fn1	-1.2906	Mm.193099	NM_010233
Hapln1	6.5979	Mm.266790	NM_013500
Hc	2.0734	Mm.2168	NM_010406
Icam1	-2.6537	Mm.435508	NM_010493
Itga2	-1.3736	Mm.5007	NM_008396
Itga3	1.1503	Mm.57035	NM_013565
Itga4	-1.8125	Mm.31903	NM_010576
Itga5	1.1826	Mm.16234	NM_010577
Itgae	1.9616	Mm.96	NM_008399
Itgal	2.0734	Mm.1618	NM_008400
Itgam	-5.0211	Mm.262106	NM_008401
Itgav	1.8947	Mm.227	NM_008402
Itgax	-3.6757	Mm.22378	NM_021334

Itgb1	1.456	Mm.263396	NM_010578
Itgb2	-7.1503	Mm.1137	NM_008404
Itgb3	-1.8378	Mm.87150	NM_016780
Itgb4	2.0734	Mm.213873	NM_001005608
Lama1	2.8719	Mm.303386	NM_008480
Lama2	5.3221	Mm.256087	NM_008481
Lama3	1.1663	Mm.42012	NM_010680
Lamb2	1.5284	Mm.425599	NM_008483
Lamb3	-1.1392	Mm.435441	NM_008484
Lamc1	-1.9972	Mm.1249	NM_010683
Mmp10	2.734	Mm.14126	NM_019471
Mmp11	2	Mm.4561	NM_008606
Mmp12	2.117	Mm.2055	NM_008605
Mmp13	1.3491	Mm.5022	NM_008607
Mmp14	-1.8895	Mm.280175	NM_008608
Mmp15	1.0512	Mm.217116	NM_008609
Mmp1a	2.2	Mm.156952	NM_032006
Mmp2	-1.8378	Mm.29564	NM_008610
Mmp3	1.4359	Mm.4993	NM_010809
Mmp7	2.0734	Mm.4825	NM_010810
Mmp8	2.7431	Mm.16415	NM_008611
Mmp9	2.5883	Mm.4406	NM_013599
Ncam1	-1.1157	Mm.4974	NM_010875
Ncam2	2.3548	Mm.433941	NM_010954
Pecam1	2.3006	Mm.343951	NM_008816
Postn	1.2501	Mm.236067	NM_015784
Sell	2.022	Mm.1461	NM_011346
Selp	-1.0056	Mm.3337	NM_011347
Sgce	3.487	Mm.8739	NM_011360
Sparc	-1.2041	Mm.291442	NM_009242
Spock1	2.0734	Mm.379020	NM_009262
Spp1	3.1866	Mm.288474	NM_009263
Syt1	2.3486	Mm.289702	NM_009306
Tgfbi	2.7034	Mm.14455	NM_009369
Thbs1	1.2243	Mm.4159	NM_011580
Thbs2	-1.6335	Mm.26688	NM_011581
Thbs3	4.6012	Mm.2114	NM_013691
Timp1	2.0734	Mm.8245	NM_011593
Timp2	1.2763	Mm.206505	NM_011594
Timp3	2.2377	Mm.4871	NM_011595
Tnc	-1.0056	Mm.454219	NM_011607
Vtn	2.0734	Mm.3667	NM_011707
Gusb	-3.6503	Mm.3317	NM_010368
Hprt	1.7076	Mm.299381	NM_013556
Hsp90ab1	1.1991	Mm.2180	NM_008302
Gapdh	1.5605	Mm.343110	NM_008084

Actb	1.1423	Mm.328431	NM_007393
Atf2	-1.7802	Mm.209903	NM_009715
Bax	2.7856	Mm.19904	NM_007527
Bcl2	3.4774	Mm.257460	NM_009741
Bcl2l1	-1.3585	Mm.238213	NM_009743
Naip1	-5.4339	Mm.6898	NM_008670
Birc2	-1.3031	Mm.335659	NM_007465
Birc3	-4.6654	Mm.2026	NM_007464
Birc5	-2.4318	Mm.8552	NM_009689
Bmp2	-1.1663	Mm.103205	NM_007553
Bmp4	-1.0882	Mm.6813	NM_007554
Brca1	1.5779	Mm.244975	NM_009764
Ccl2	3.4295	Mm.290320	NM_011333
Ccl20	-5.4339	Mm.116739	NM_016960
Ccnd1	-1.1503	Mm.273049	NM_007631
Cd5	-6.1988	Mm.779	NM_007650
Cdk2	-2.3653	Mm.111326	NM_016756
Cdkn1a	2.1111	Mm.195663	NM_007669
Cdkn1b	-5.7837	Mm.2958	NM_009875
Cdkn2a	1.0483	Mm.4733	NM_009877
Cdkn2b	1.0483	Mm.423094	NM_007670
Cebpb	1.1392	Mm.439656	NM_009883
Csf2	-4.7966	Mm.4922	NM_009969
Cxcl1	-4.7634	Mm.21013	NM_008176
Cxcl9	-10.4977	Mm.766	NM_008599
Cyp19a1	-3.5357	Mm.5199	NM_007810
Egr1	-5.4717	Mm.181959	NM_007913
Ei24	1.2294	Mm.4337	NM_007915
En1	-5.4339	Mm.2657	NM_010133
Fas	-4.8973	Mm.1626	NM_007987
Fasl	-5.4339	Mm.3355	NM_010177
Fasn	-1.1991	Mm.236443	NM_007988
Fgf4	-5.4339	Mm.4956	NM_010202
Fn1	3.0063	Mm.193099	NM_010233
Fos	-27.7036	Mm.246513	NM_010234
Foxa2	-2.5175	Mm.938	NM_010446
Gadd45a	2.528	Mm.72235	NM_007836
Greb1	-1.9346	Mm.428062	NM_015764
Gys1	-1.1826	Mm.275654	NM_030678
Hhip	-5.4339	Mm.254493	NM_020259
Hk2	4.9178	Mm.255848	NM_013820
Hoxa1	-12.3121	Mm.197	NM_010449
Hsf1	1.5779	Mm.347444	NM_008296
Hspb1	-1.8302	Mm.13849	NM_013560
Icam1	-4.4444	Mm.435508	NM_010493
Igfbp3	-1.5605	Mm.29254	NM_008343

Igfbp4	-11.5675	Mm.233799	NM_010517
Ikbkb	9.1769	Mm.277886	NM_010546
Il1a	-2.1916	Mm.15534	NM_010554
Il2	-14.6416	Mm.14190	NM_008366
Il2ra	-5.4339	Mm.915	NM_008367
Il4ra	-18.6616	Mm.233802	NM_001008700
Irf1	-12.5708	Mm.105218	NM_008390
Jun	-3.1645	Mm.275071	NM_010591
Lef1	-6.242	Mm.255219	NM_010703
Lep	-1.8687	Mm.277072	NM_008493
Lta	-5.4339	Mm.87787	NM_010735
Mdm2	-1.1266	Mm.22670	NM_010786
Mmp10	-5.4339	Mm.14126	NM_019471
Mmp7	-5.4339	Mm.4825	NM_010810
Myc	2.2784	Mm.2444	NM_010849
Nab2	-2.6611	Mm.336898	NM_008668
Nfkbia	-2.3166	Mm.170515	NM_010907
Nos2	2.3916	Mm.2893	NM_010927
Nrip1	1.3177	Mm.74711	NM_173440
Odc1	-2.4829	Mm.34102	NM_013614
Pparg	-3.2535	Mm.3020	NM_011146
Ptch1	-1.9889	Mm.228798	NM_008957
Ptgs2	-1.3031	Mm.292547	NM_011198
Rbp1	-2.912	Mm.279741	NM_011254
Sele	-22.3469	Mm.5245	NM_011345
Selp	2.2942	Mm.3337	NM_011347
Tank	-1.2763	Mm.244393	NM_011529
Tcf7	-1.9212	Mm.31630	NM_009331
Tert	-1.3398	Mm.10109	NM_009354
Tfrc	-21.2885	Mm.28683	NM_011638
Pmepa1	1.567	Mm.73682	NM_022995
Tnf	-3.0568	Mm.1293	NM_013693
Trp53	1.8506	Mm.222	NM_011640
Vcam1	-3.8424	Mm.76649	NM_011693
Vegfa	1.7029	Mm.282184	NM_009505
Wisp1	-1.3585	Mm.10222	NM_018865
Wnt1	-1.8302	Mm.1123	NM_021279
Wnt2	-5.4339	Mm.33653	NM_023653
Gusb	-1.3775	Mm.3317	NM_010368
Hprt	-2.3817	Mm.299381	NM_013556
Hsp90ab1	1.0629	Mm.2180	NM_008302